



Three-Dimensional Bearing Capacity Analysis of Rock Foundations Subjected to the Loads of Gravity Dams, Case Study: Shafaroud Dam

H. AlKhafaji¹, M. Imani^{2*}, A. Fahimifar¹

¹Department of Civil and Environmental Engineering, Amirkabir University of Technology, Tehran, Iran.

²Geotechnical Engineering Group, Amirkabir University of Technology, Garmsar Campus, Garmsar, Iran.

ABSTRACT: The effect of seepage on the bearing capacity of soils was investigated by different researchers, while this special subject in the field of rock foundations has not been thoroughly investigated by researchers. Moreover, rock foundations are commonly required for large structures, like bridges and dams in which, seepage forces exist. Because of the complicated loading conditions of such large structures, using the simple available 2D methods for determining the bearing capacity may not give accurate results. In this paper, the ultimate bearing capacity of rock masses subjected to loads of gravity dams was investigated using the 3D finite element method. A case study of the Shafaroud concrete dam, which is under construction on a rock mass, was considered and the effect of seepage through the rock foundation was investigated using the numerical models. The bearing capacity was obtained by applying incremental stress to the bedding rock mass. For improving the accuracy of the obtained bearing capacity, the area of the rock mass in contact with the dam base was divided into some parts and uniform incremental stresses were applied to each part. This method resulted in the highest possible accuracy in obtaining the bearing capacity of dam foundations. The comparison of the obtained results and the available solutions showed good conformity among them. The suggested method is an appropriate guideline for determining the ultimate bearing capacity of foundations with complicated geometry and loading conditions.

Review History:

Received: Apr. 17, 2020

Revised: May, 26, 2020

Accepted: Jun. 13, 2020

Available Online: Jun. 23, 2020

Keywords:

Rock mass

Hoek–Brown

Bearing capacity

Three dimensional

Seepage

1- Introduction

The experimental data show that most rock masses behave nonlinearly in nature. Because of this nonlinearity, different researchers did not focus on the bearing capacity of rock masses as much as soil beddings. Among the available researches in this field, the studies performed by Clausen [1], Bindlish, Singh, and Samadhiya [2] and Javid, Fahimifar, and Imani [3] can be mentioned, which are about applying distinct element methods on determining the ultimate bearing capacity of rock foundations. Also, Mansouri, Imani, and Fahimifar [4] investigated the ultimate bearing capacity of rock masses considering the non-linear Hoek–Brown criterion using three-dimensional finite element analyses. Some analytical methods are also existed in the literature, among others, the studies performed by Yang and Yin [5], Merifield, Lyamin and Sloan [6], Saada, Maghous and Garnier [7], and Mao, Al-Bittar and Soubra [8] can be mentioned. However, few studies like Imani, Fahimifar, and Sharifzadeh [9] and Imani [10] considered the effect of joint sets on failure mode and ultimate bearing capacity of rock foundations. In a recent paper, the effect of seepage on the bearing capacity of rock masses was investigated by AlKhafaji, Imani, and Fahimifar

[11]. They used the kinematic approach of limit analysis using the Hoek-Brown failure criterion for the rock mass. The effect of seepage was considered by non-dimensional ratio, $i(\gamma_w/\gamma_{sub})$, where, i is the hydraulic gradient, and γ_w and γ_{sub} refer to the unit weights of water and submerged rock mass, respectively. It is worth noting that most available methods for determining the ultimate bearing capacity of rock masses were suggested for a two-dimensional section of a strip footing or a simple three-dimensional geometry of footing which are subjected to simple loading configurations, i.e., only vertical loading from the superstructure. These simple methods are not applicable for the foundation of the structures like dams, which are complicated in both geometry and the loading conditions.

In this paper, a full 3D model of the Shafaroud concrete dam, which is under construction in Guilan province, north of Iran, was constructed using PLAXIS 3D software and the ultimate bearing capacity of its foundation was determined. Both cases of ignoring/considering the seepage were considered in the modeling. Because of the non-uniform distribution of the stress on the underlying rock mass, an elaborate method was used for obtaining the stress-settlement behavior and the corresponding ultimate bearing capacity of the rock mass beneath the dam. Finally, comparisons between

*Corresponding author's email: imani@aut.ac.ir



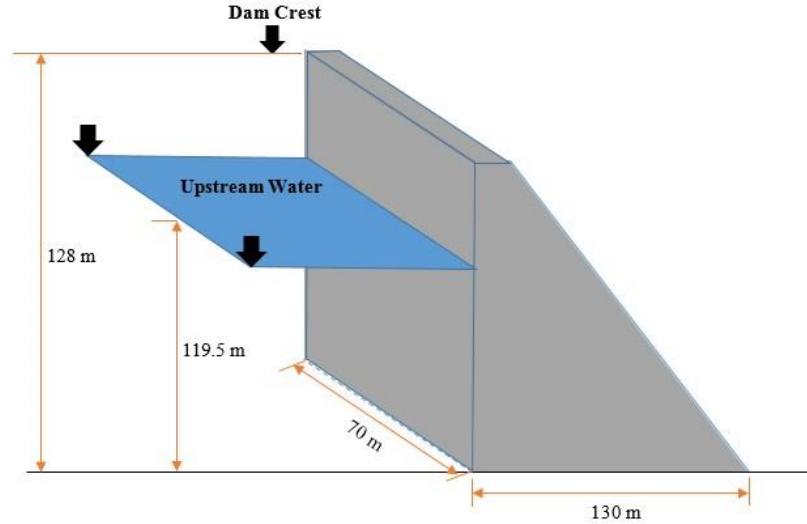


Fig. 1. Shafaroud dam view and the upstream water level.

the obtained results with those available in the literature were presented and the effect of different parameters on the bearing capacity was also investigated.

2- The Hoek-Brown Failure Criterion

The 2002 edition of the Hoek-Brown failure criterion [12] for rock masses is as follows:

$$\sigma_1' = \sigma_3' + \sigma_{ci} \left(m_b \frac{\sigma_3'}{\sigma_{ci}} + s \right)^a \quad (1)$$

Where σ_1' and σ_3' are the major and minor principal stresses at failure, σ_{ci} is the uniaxial compressive strength of the intact rock, and m_b is given by:

$$m_b = m_i \exp\left(\frac{GSI - 100}{28 - 14D}\right) \quad (2)$$

In which, m_i is a constant parameter for the intact rock and can be obtained from the experiments, GSI is the geological strength index of the rock mass and D is a factor that depends upon the degree of disturbance of the rock mass which varies from zero for undisturbed in situ rock masses to 1 for very disturbed rock masses. s and a are constants for the rock mass given by the following relationships:

$$s = \exp\left(\frac{GSI - 100}{9 - 3D}\right) \quad (3)$$

$$a = \frac{1}{2} + \frac{1}{6} \left(e^{\frac{GSI}{15}} - e^{\frac{20}{3}} \right) \quad (4)$$

This failure criterion which has been implemented in some commercial software, like PLAXIS 3D, was used in the present paper for the dam rock foundation.

3- The Shafaroud Dam Data

3- 1- Dam geometry

Fig. 1 shows the 128 meters height, 70 meters length, and 130 meters width (B) roller compacted concrete (RCC) dam, named Shafaroud, which is under construction in Guilan Province, north of Iran. Based on the hydrological studies, the height of the upstream water in the normal condition is equal to 119.5 meters [13]. The dam site is shown in Fig. 2.

3- 2- Material Properties

The geotechnical investigation shows that the foundation material is composed of a thick layer of micro conglomerate and tuff sandstone with siltstone interlayers. Fig. 3 shows the layering of the rock mass beneath the dam body. The properties of the rock mass were presented in Table 1.

4- Numerical Modeling

4- 1- Optimum mesh and model size

The results of numerical analyses are highly affected by the size of the meshes and the model domain. For optimizing these values, sensitivity analyses were performed. The best value for the size of the mesh and the dimensions of the domain was determined by trial and error, presenting no significant changes in the results if the mesh size is reduced or the model dimensions are increased. The final domain and mesh size used in the present study is shown in Fig. 4.



Fig. 2. Location of the Shafaroud dam (37° 32' N and 49° 08' E).

Table 1. Properties of the rock mass foundation of the Shafaroud dam [13].

Layer	Name	γ_{sat} (kN/m ³)	σ_{ci} (MPa)	m_i	GSI	D	Poisson's ratio
1	Micro conglomerate	26	73	21	33	0	0.29
2	Tuff sandstone with siltstone	25	54	17	30	0	0.31

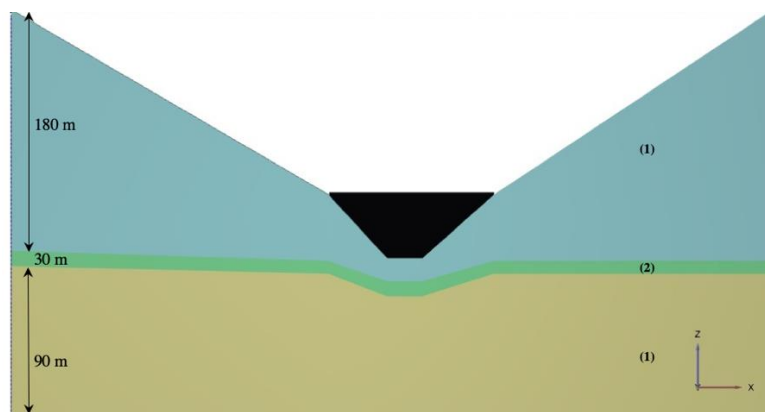


Fig. 3. The rock mass layers surround the Shafaroud dam.

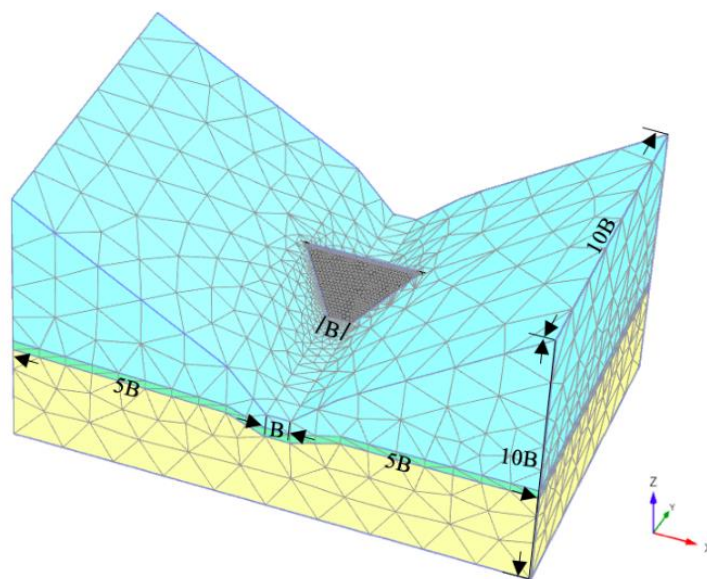


Fig. 4. 3D Numerical model of the Shafaroud dam layers and problem geometry.

4- 2- Boundary Condition

In the numerical models, two different cases, including dry rock mass and the rock mass subjected to seepage were modeled. The base of the models was constrained in three directions and the side boundaries were fixed in two directions in a way that vertical displacements were allowed. The contact surface of the dam base and the bedrock was considered to be rough. For this purpose, the nodes under the dam foundation were fixed in the horizontal direction.

4- 3- Obtaining the stress-settlement curve for the dam foundation

4- 3- 1- The method used

The stress-settlement curve is usually used for obtaining the bearing capacity. This curve can be obtained by applying incremental stress to the foundation material and recording the corresponding settlement. This procedure can be performed in the field by plate load test or more simply, by using numerical software that the latter was applied in the current research.

In the case of a simple shallow foundation subjected to a central vertical load, one can easily apply an incremental uniformly distributed stress to the bedding material and obtain the corresponding settlements. But in a foundation of a gravity dam that is subjected to non-uniform stresses from its body weight, upstream water, and multi-directional seepage, the stress distribution exerted to the foundation material is too complicated and its magnitude in different parts of the base foundation is difficult to be anticipated. Therefore, in the current study, the numerical analysis of bearing capacity comprises two steps. In the first step, some full 3D models were constructed considering different values of $i(\gamma_w/\gamma_{sub})$. Then, the stress distribution and magnitude applied to the contact surface exactly beneath the dam body were obtained.

It is evident that the stress beneath the dam is not uniform and it comprises different components in the X, Y, and Z directions. In the second step, keeping fixed the ratio of these components and omitting the dam body, different incremental stress values in X, Y, and Z directions were applied to the contact surface of the dam and its base foundation, and the corresponding settlements were obtained. These data were used for drawing the load-settlement curve.

4- 3- 2- Stress distribution and the stress-settlement curve for the Shafaroud dam foundation

For performing the first step described in the previous section, three different values of $i(\gamma_w/\gamma_{sub})$ were considered, which include zero, 0.3, and 0.6. The Cartesian coordinate system and the positive stress directions used in the PLAXIS 3D were shown in Fig. 5. Based on this figure, the stress component, σ'_{zz} is normal to the rock mass beneath the dam body, while the components σ'_{zx} and σ'_{zy} are the surface tractions that are applied to the contact surface of the dam body and underlying rock mass. These stress components were used in this paper for obtaining the stress-settlement curve and the corresponding ultimate bearing capacity.

As an example, Fig. 6 shows the stress contours of the rock mass beneath the dam body, for the case of $i(\gamma_w/\gamma_{sub})=0.6$. This figure clearly shows that the stress exerted on the rock foundation is not uniform. Therefore, for applying incremental stress to this surface to obtain the stress-settlement curve, it is necessary to divide it into some parts in each of them, a uniform distribution of stress exists. Since the stress intensity is changeable in the base of the dam, it is essential to consider the partitions in a way that the variation of the stress components in each part be ignorable. For the sake of simplicity, this partitioning was performed considering the lowest possible variation in the normal

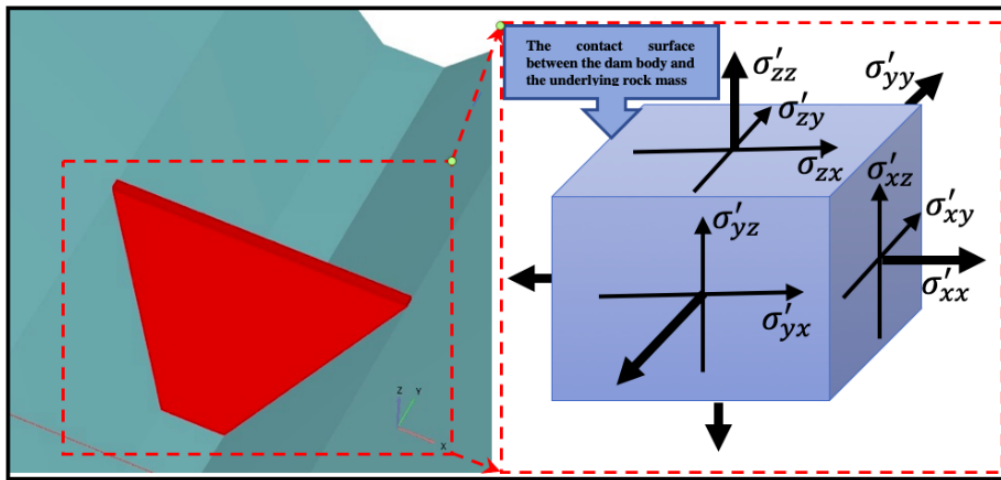


Fig. 5. The Cartesian coordinate system and the positive stress directions based on the PLAXIS 3D default.

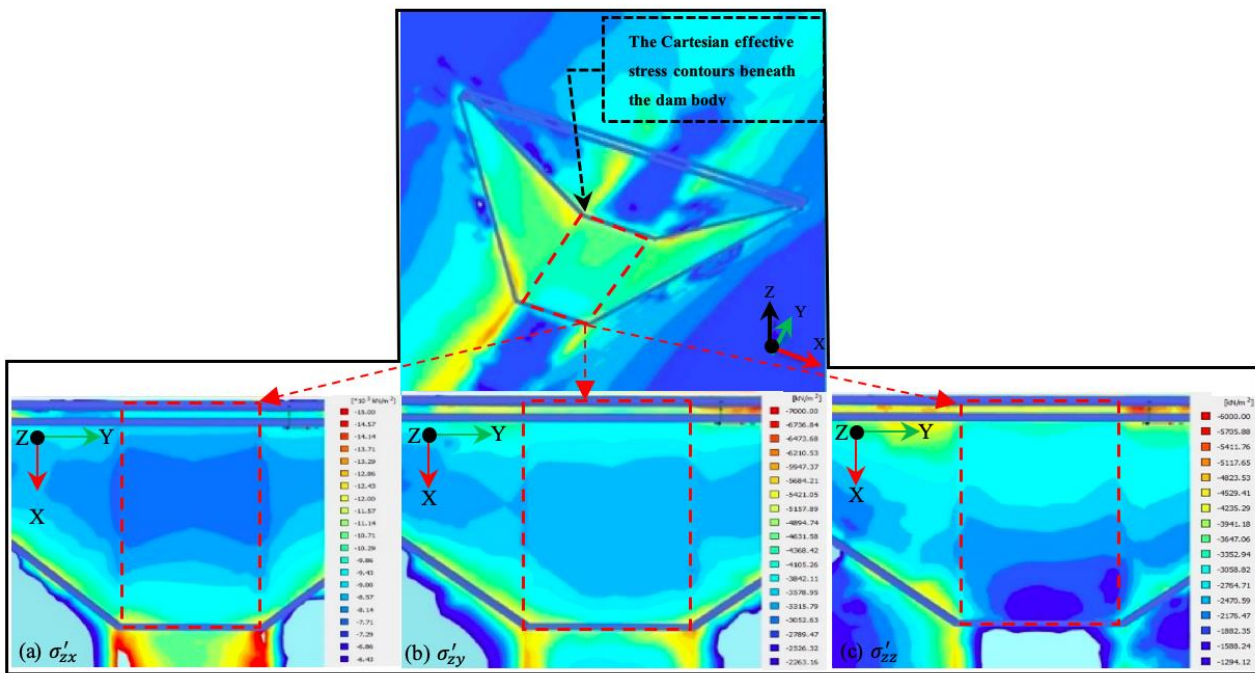


Fig. 6. The Cartesian effective stress contours beneath the dam body in the X-Y plane, assuming $i(\gamma_w/\gamma_{sub})=0.6$.

stress component, σ'_{zz} , and the surface tractions σ'_{zx} and σ'_{zy} , simultaneously. As an example, Fig. 7 shows the partitioning of the base foundation for the case of $i(\gamma_w/\gamma_{sub})=0.6$. For this particular case, the base foundation was divided into six parts in each of them, the intensity of the stress components σ'_{zz} , σ'_{zx} , σ'_{zy} , does not have considerable variations. Based on the stress variations exerted to the rock foundation, for all considered magnitudes of the $i(\gamma_w/\gamma_{sub})$ ratio, six partitions were considered. The magnitude of the stress components in

each partition was presented in Table 2. The negative sign shows that the direction of the stress component is opposite to the convention shown in Fig. 5.

For obtaining the stress-settlement curve, keeping fixed the ratio among the stress components of Table 2, the incremental stress value for the three directions, i.e., σ'_{zz} , σ'_{zx} , σ'_{zy} , were applied to each part of the foundation, simultaneously and the corresponding stress-settlement curves were obtained for each part.

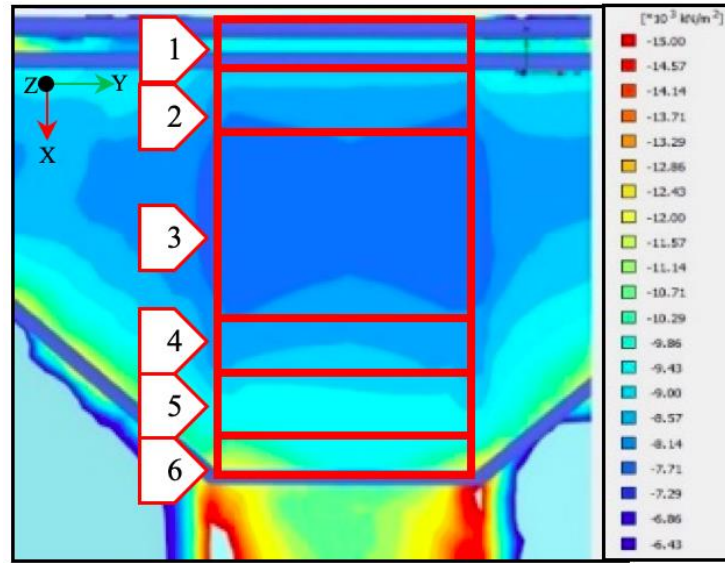


Fig. 7. The dam foundation base divided into different parts of the same σ'_{zx} , considering $i(\gamma_w/\gamma_{sub})=0.6$.

Table 2. The Cartesian effective stress components for each part of the dam foundation base for different values of $i(\gamma_w/\gamma_{sub})$.

$i(\gamma_w/\gamma_{sub})$	Cartesian Effective Stress Components (MPa)	Parts					
		1	2	3	4	5	6
0	σ'_{zz}	-4.6	-4	-3.2	-2.9	-2.3	-1.8
	σ'_{zx}	-10.5	-8.5	-7.5	-8.5	-9.5	-11
	σ'_{zy}	-5.7	-4.2	-3.6	-3.6	-3.7	-4.2
0.3	σ'_{zz}	-4.2	-3.6	-2.75	-2.25	-2	-1.6
	σ'_{zx}	-9.5	-8	-7.25	-8	-8.75	-10
	σ'_{zy}	-4.9	-4.1	-3.5	-3.5	-3.7	-4.15
0.6	σ'_{zz}	-3.8	-3	-2.5	-2.5	-1.7	-1.4
	σ'_{zx}	-9	-8.5	-8	-8.5	-8.7	-9.5
	σ'_{zy}	-4.5	-3.5	-2.75	-2.75	-3.5	-4

5- Results and Discussion

5- 1- Determining the stress-settlement curve and the corresponding ultimate bearing capacity

Lutenegger and Adams [14] discussed four methods for obtaining ultimate bearing capacity using the stress-settlement curve, which include tangent intersection, Log-Log, hyperbolic, and 0.1B methods. Each one of these methods may give a different value of bearing capacity. In the present study, all these methods were considered for obtaining the bearing capacity of the Shafaroud dam foundation and the method, which resulted in the lowest bearing capacity was

chosen. The results obtained for different parts of the dam foundation show that the tangent-intersection method results in the lowest bearing capacity. Based on the discussions presented in the previous section, and as shown in Fig. 7, the rock foundation was divided into six parts; for each of them, the vertical stress, σ'_{zz} , - settlement curve was obtained. For getting the best results, three curves were obtained for each part, one for the middle and the two others for the right and left sides of the parts. In each part, the curve which resulted in the lowest bearing capacity was selected as the representative vertical stress-settlement curve for the part.

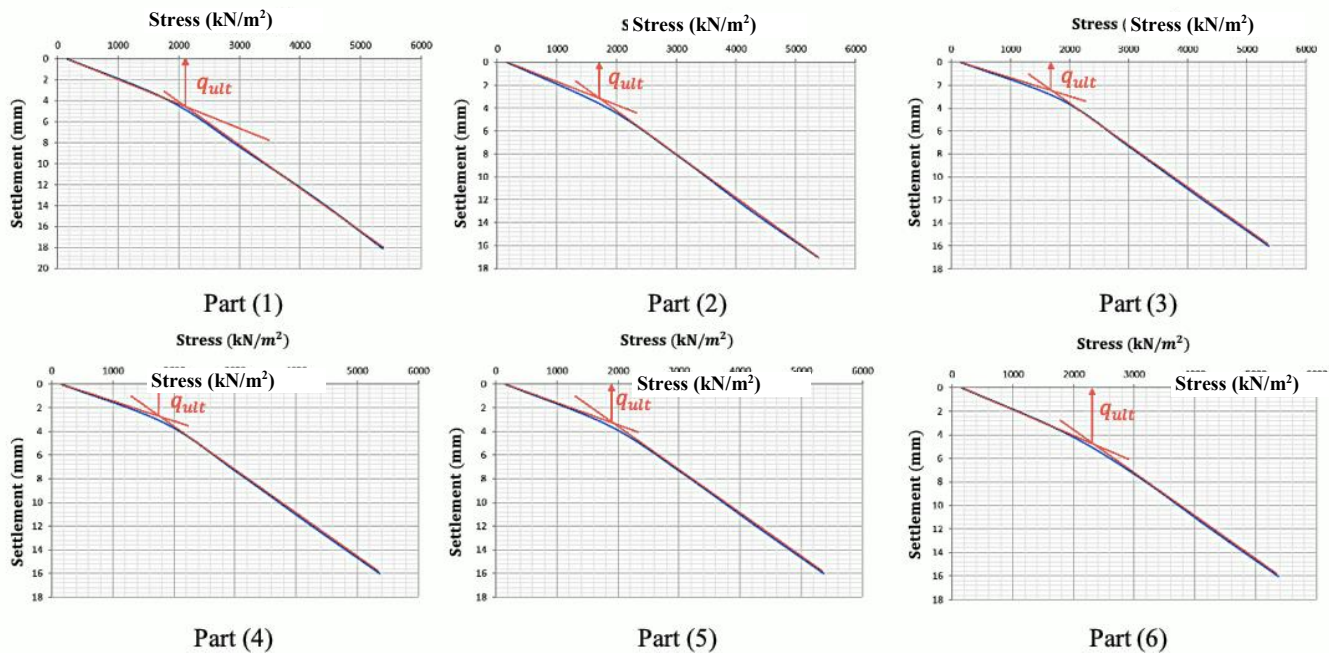


Fig. 8. The vertical stress-settlement curve corresponded to the lowest q_u in the rock foundation, considering different parts of $i(\gamma_w/\gamma_{sub})=0.3$.

Table 3. The ultimate bearing capacity for each part of the dam foundation based on different values of $i(\gamma_w/\gamma_{sub})$ in the case of dam foundation.

Shafaroud dam foundation							
$i(\gamma_w/\gamma_{sub})$	Ultimate Bearing Capacity	Part					
		1	2	3	4	5	6
0	q_u (MPa)	3.95	3.60	3.40	3.50	3.75	4.05
0.3	q_u (MPa)	2.05	1.85	1.70	1.75	1.90	2.15
0.6	q_u (MPa)	1.65	1.40	1.20	1.30	1.50	1.75

Fig. 8 shows the vertical stress-settlement curve for each considered part of the rock foundation, considering $i(\gamma_w/\gamma_{sub})=0.3$. The application of the tangent-intersection method was also shown in each curve. For all considered $i(\gamma_w/\gamma_{sub})$ values, the lowest bearing capacity, q_u , in each part was determined and was presented in Table 3. As can be seen, part 3 has the smallest bearing capacity among the others. Since it is not possible to introduce six ultimate bearing capacities for the rock foundation, the lowest q_u among the six partitions was selected as the final ultimate bearing capacity. Fig. 9 shows the vertical stress-settlement curve, which resulted in the lowest q_u for different $i(\gamma_w/\gamma_{sub})$ ratios.

5- 2- Comparison with the existing solutions

AlKhafaji, Imani, and Fahimifar [11] proposed upper bound solutions to the bearing capacity of rock masses in the

dry case and also with considering the seepage effects. To the authors' knowledge, their method is the only published solution that deals with the effect of seepage on the bearing capacity of rock masses. By considering a failure mechanism shown in Fig. 10, they developed Eq. (5) for determining the ultimate bearing capacity of rock masses subjected to seepage.

$$q_u^S = s^{0.5} \sigma_{ci} N_\sigma^S + q_0 N_q^S + \frac{\gamma B}{2} N_\gamma^S \quad (5)$$

Where q_u^S is the bearing capacity of rock masses subjected to seepage, q_0 is the surcharge load, γ is the density of the rock mass, B is the foundation width, and N_σ^S , N_q^S , and N_γ^S are

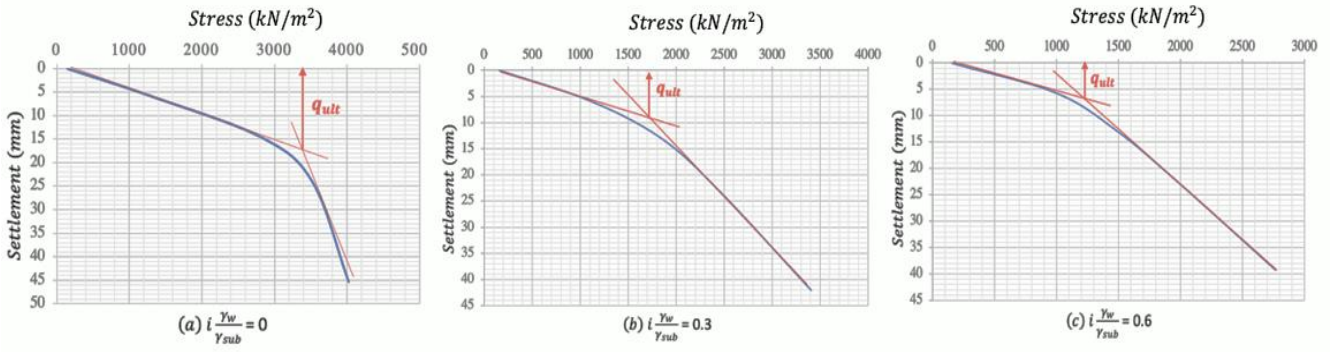


Fig. 9. The vertical stress-settlement curve corresponded to the lowest q_u in the rock foundation, considering the different values of $i(\gamma_w/\gamma_{sub})$.

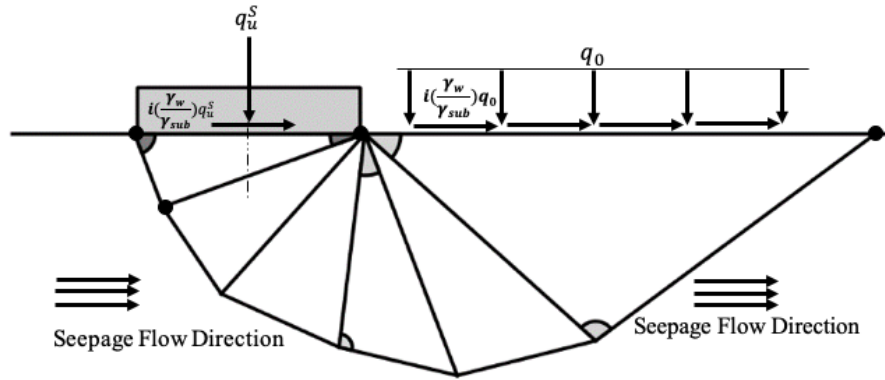


Fig. 10. The failure mechanism considered by AlKhafaji, Imani, and Fahimifar [11] for determining the bearing capacity of rock masses subjected to seepage.

the bearing capacity factors in the presence of water seepage. Based on the AlKhafaji, Imani, and Fahimifar [11] method, the general form of the bearing capacity formula for dry rock masses is also as follows:

$$q_u = s^{0.5} \sigma_{ci} N_\sigma + q_0 N_q + \frac{\gamma B}{2} N_\gamma \quad (6)$$

Where q_u is the bearing capacity of dry rock masses and N_σ , N_q and N_γ are the bearing capacity factors for dry rock masses.

In the present paper, the effect of seepage on the bearing capacity of rock masses was proposed as a dimensionless factor, named the seepage factor, which can be obtained as follows:

$$\xi = \frac{q_u^S}{q_u} \quad (7)$$

This dimensionless factor can be calculated for the Shafaroud dam foundation using both the numerical analyses presented in the current paper and the upper bound method presented by AlKhafaji, Imani, and Fahimifar [11]. It should be noted that in calculating the ξ factor from the results of the present paper, i.e., numerical modeling, the numerator of Eq. (7) was obtained assuming $i(\gamma_w/\gamma_{sub}) \neq 0$, while the denominator was obtained assuming $i(\gamma_w/\gamma_{sub}) = 0$. Also, for further validation, the method presented by Veiskarami and Habibagahi [16] was also used for comparison. They proposed an upper bound approach for determining the effect of seepage on the bearing capacity of soils. For the

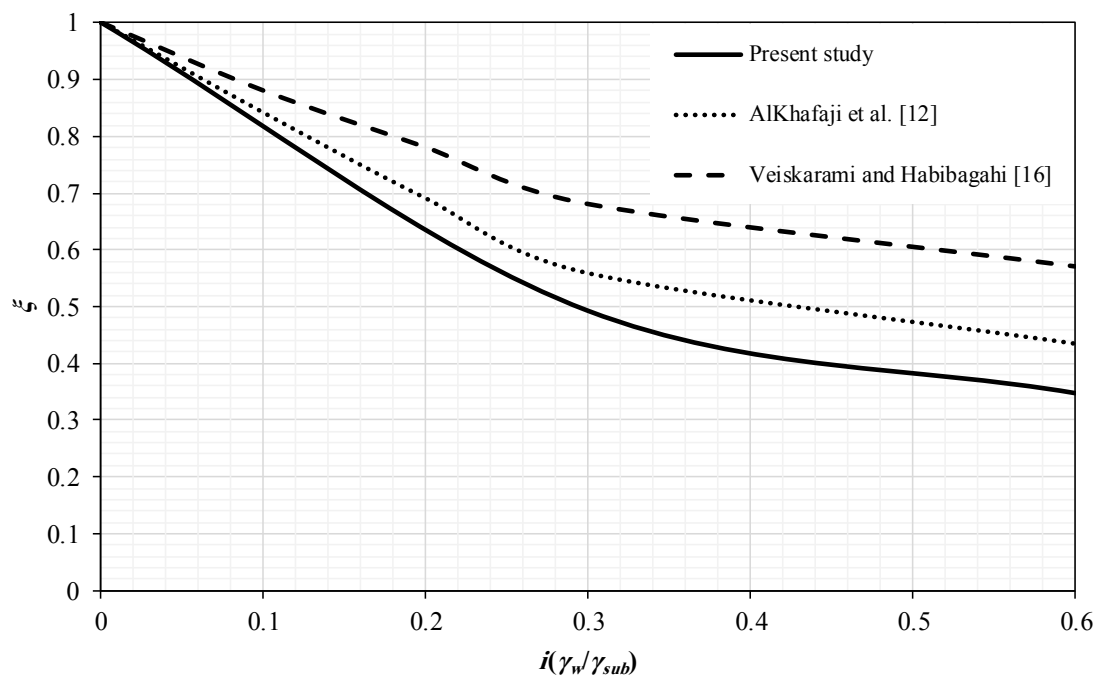


Fig. 11. Comparison between the upper bound method and numerical method using PLAXIS 3D results for Shafaroud dam foundation.

possibility of the results comparison of the present study with a method that is based on soil media, the equivalent Mohr-Coulomb properties of the Shafaroud dam were determined using the formulations presented by Hoek, Carranza-Torres and Corkum [12]. Then, these magnitudes were used in the bearing capacity formulations proposed by Veiskarami and Habibagahi [15].

Fig. 11 shows a comparison between the ξ factor obtained from the present study and that obtained from the AlKhafaji, Imani and Fahimifar [11] and Veiskarami and Habibagahi [15] upper bound methods. It can be seen that the trend of variation of ξ versus $i(\gamma_w/\gamma_{sub})$ is similar in all methods. Also, the numerical analyses presented in the current paper resulted in smaller ξ values, which means smaller q_u^S . Therefore, in practical applications, using the results of the 3D numerical simulations are on the safe side.

It should be noted that although the results of the present paper are based on some elaborated 3D numerical models and the methods proposed by AlKhafaji, Imani and Fahimifar [11] and Veiskarami and Habibagahi [15] are based on some 2D analytical calculations, not great differences were observed between the seepage factor obtained from these two methods. This is due to the approximate plane strain condition that existed in long structures like gravity dams. However, the results of the available 2D methods may not be useful in the structures in which the plane strain conditions do not exist, like arch dams. More researches are required in such structures.

5- 3- Sensitivity Analyses

Considering different magnitudes of the input parameters, sensitivity analyses were performed to obtain the q_u^S for the Shafaroud dam foundation. Fig. 12 shows the variation of ultimate bearing capacity, q_u^S versus $i(\gamma_w/\gamma_{sub})$, considering different values of GSI and m_i . It can be seen that by increasing m_i , the bearing capacity increased. Also, increasing $i(\gamma_w/\gamma_{sub})$ resulted in decreasing q_u^S . The rate of this reduction is more sensible for $i(\gamma_w/\gamma_{sub}) < 0.3$, while for the $i(\gamma_w/\gamma_{sub}) > 0.3$, the rate of reduction of q_u^S became negligible, especially for the rock masses with a high value of GSI.

6- Conclusion

The results of numerical analyses of the Shafaroud dam foundation subjected to seepage forces showed:

The most available methods for determining the bearing capacity are based on simple foundation geometries that are subjected to simple loadings. As shown in the present paper, these methods may not be appropriate for the foundations which are subjected to complicated loadings, like the foundation of a gravity dam. Numerical methods are useful in such cases.

Due to the existence of seepage through the dam foundation, the bearing capacity was not reduced considerably. Considering different properties for the rock mass foundation, by increasing $i(\gamma_w/\gamma_{sub})$ from zero to 0.6, the bearing capacity was reduced in the range of 60% to 70%.

The obtained results show that in long structures like

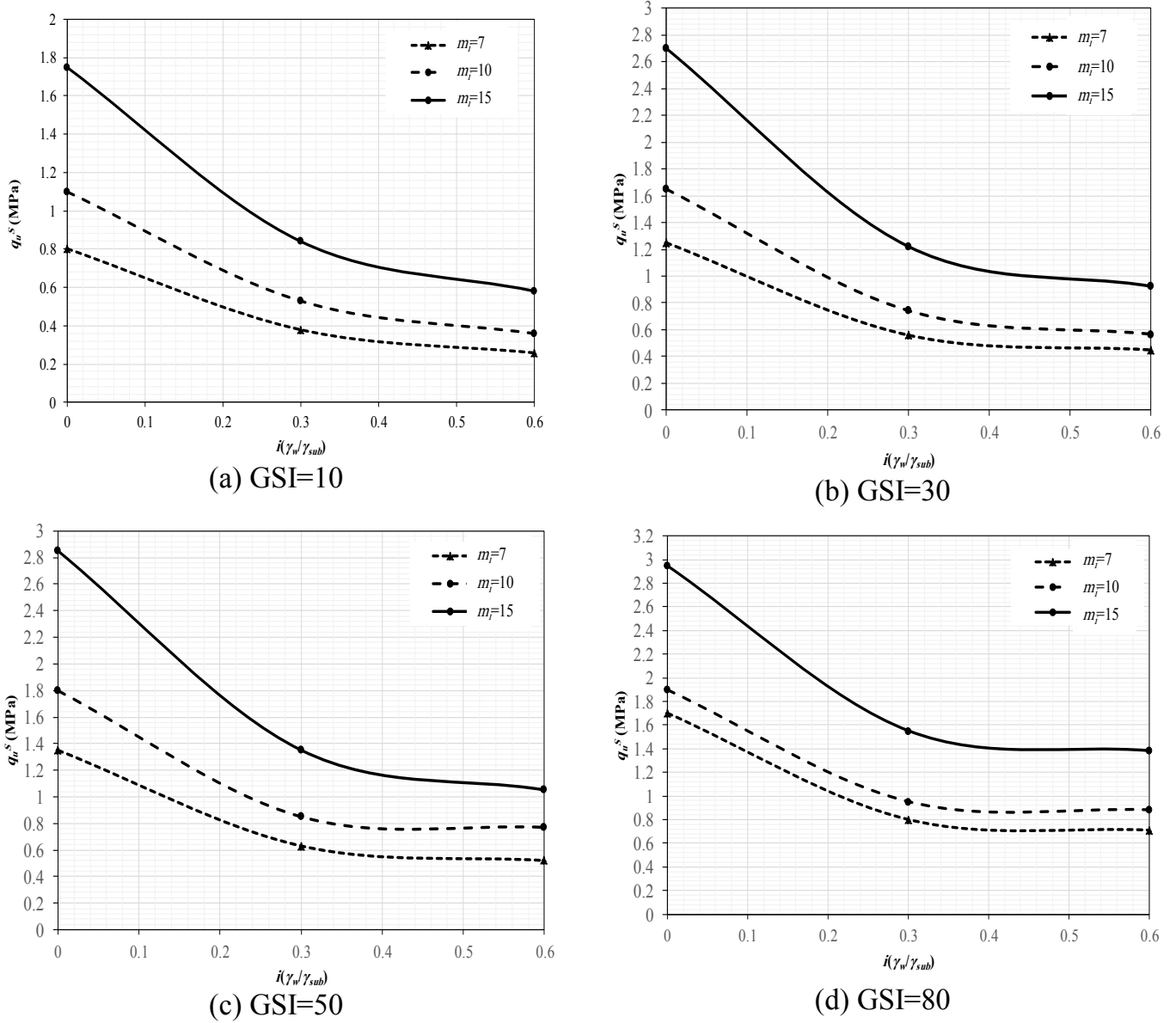


Fig. 12. Ultimate bearing capacity of Shafaroud dam foundation subjected to seepage considering different values of m_i and GSI.

gravity dams, the existing 2D methods result in almost appropriate bearing capacities since the plane strain conditions are governed.

The procedure used in the present paper for obtaining the bearing capacity is appropriate in the foundations which are subjected to non-uniform stresses.

References

- [1] J. Clausen, Bearing capacity of circular footings on a Hoek—Brown material, *International journal of rock mechanics and mining sciences* (1997), 57 (2013) 34-41.
- [2] A. Bindlish, M. Singh, N. Samadhiya, Modeling of ultimate bearing capacity of shallow foundations resting on jointed rock mass, *Indian Geotechnical Journal*, 43(3) (2013) 251-266.
- [3] Javid, A. Fahimifar, M. Imani, Numerical Studies on the Bearing Capacity of two Interfering Strip Footings based on Hoek—Brown Materials, in: 13th ISRM International Congress of Rock Mechanics, International Society for Rock Mechanics and Rock Engineering, 2015.
- [4] M. Mansouri, M. Imani, A. Fahimifar, Ultimate bearing capacity of rock masses under square and rectangular footings, *Computers and Geotechnics*, 111 (2019) 1-9.
- [5] X.-L. Yang, J.-H. Yin, Upper bound solution for ultimate bearing capacity with a modified Hoek—Brown failure criterion, *International Journal of Rock Mechanics and Mining Sciences*, 42(4) (2005) 550-560.
- [6] R.S. Merifield, A.V. Lyamin, S. Sloan, Limit analysis solutions for the bearing capacity of rock masses using the generalized Hoek—Brown criterion, *International Journal of Rock Mechanics and Mining Sciences*, 43(6) (2006) 920-937.
- [7] Z. Saada, S. Maghous, D. Garnier, Bearing capacity of shallow foundations on rocks obeying a modified Hoek—Brown failure criterion, *Computers and Geotechnics*, 35(2) (2008) 144-154.
- [8] N. Mao, T. Al-Bittar, A.-H. Soubra, Probabilistic analysis and design of strip foundations resting on rocks obeying Hoek—Brown failure criterion, *International Journal of Rock Mechanics and Mining Sciences*, 49 (2012) 45-58.
- [9] M. Imani, A. Fahimifar, M. Sharifzadeh, Upper bound solution for the bearing capacity of submerged jointed rock foundations, *Rock mechanics and rock engineering*, 45(4) (2012) 639-646.
- [10] M. Imani, Determining Bearing Failure Modes of Jointed Rock Foundations Subjected to the Load of Strip Footings, *AUT Journal of Civil Engineering*, 3(2) (2019) 157-166.
- [11] H. AlKhafaji, M. Imani, A. Fahimifar, Ultimate Bearing Capacity of Rock Mass Foundations Subjected to Seepage Forces Using Modified Hoek—Brown Criterion, *Rock Mechanics and Rock Engineering*, 53(1) (2020) 251-268.
- [12] E. Hoek, C. Carranza-Torres, B. Corkum, Hoek-Brown failure criterion-2002 edition, *Proceedings of NARMS-Tac*, 1(1) (2002) 267-273.
- [13] Technical report of the Shafaroud dam, Mahab Ghods Inc., Tehran, 1999.
- [14] A.J. Lutenecker, M.T. Adams, Bearing capacity of footings on compacted sand, in: *Fourth International Conference on Case Histories in Geotechnical Engineering*, St. Louis, Missouri, 1998, pp. 1216-1224.
- [15] M. Veiskarami, G. Habibagahi, Foundations bearing capacity subjected to seepage by the kinematic approach of the limit analysis, *Frontiers of Structural and Civil Engineering*, 7(4) (2013) 446-455.

HOW TO CITE THIS ARTICLE

H. AlKhafaji, M. Imani, A. Fahimifar, *Three-Dimensional Bearing Capacity Analysis of Rock Foundations Subjected to the Loads of Gravity Dams, Case Study: Shafaroud Dam*, *AUT J. Civil Eng.*, 5(2) (2021) 257-268.

DOI: [10.22060/ajce.2020.18281.5671](https://doi.org/10.22060/ajce.2020.18281.5671)



